

EFFECT OF LOCALLY ENHANCED HEAT DISSIPATION OF THE POLAR ON LI-ION POWER BATTERIES

by

**Haifeng FANG^{a,b}, Jin CAO^a, Kanwen XU^{a*}, Lihua CAI^{a,b},
Haoda WU^a, and Qubiao WU^{a,b}**

^a College of Mechanical Engineering, Jiangsu University of Science and Technology,
Zhenjiang, Jiangsu, China

^b Suzhou Institute of Technology, Jiangsu University of Science and Technology,
Zhangjiagang, Jiangsu, China

Original scientific paper
<https://doi.org/10.2298/TSCI201016351F>

For the sake of comprehend the influence of locally enhanced heat dissipation of the polar on Li-Ion power batteries, coupling the thermal effect of anode and cathode, the heat generation model of Li-Ion battery with different discharge magnification is obtained. Based on this model, the discharge process simulation analysis of the single battery is carried out and compared with the experimental results. The experiment results show that battery polarity heat effect has great influence on the temperature field distribution of the battery. Then, a locally enhanced heat dissipation structure is set up near the polar region and a comparative experiment is carried out by changing the discharge rate. Although the heat pipe can only slightly improve the discharge capacity of Li-Ion battery by enhancing the heat dissipation capability of polarity, the heat generated under low discharge rate can be reduced by using the heat pipe with low emission rate, the heat generated by the polar region can be effectively and timely exported to reduce the temperature of the polar region and it can greatly reduce the overall temperature of the battery. Then, according to the thermal characteristics and the results of locally enhanced heat dissipation analysis, a new battery module is designed and simulated. The prototype is completed and tested. The results show that this method can effectively reduce the temperature rise and temperature difference of the battery module by using locally enhanced heat dissipation structure. Finally, combined with the simulation and the experimental results, some useful suggestions are put forward for the design and manufacture of battery modules and battery boxes.

Key words: *Li-Ion power battery, battery poles, battery module, heat pipe, locally enhanced heat dissipation*

Introduction

Compared with other types of high energy density, no memory effect, low self-discharge rate, high voltage and so on are the advantages of Lithium-Ion (Li-Ion) batteries [1], and are extensively used in hand-held devices for instance mobile phones, netbooks, and video cameras. In recent years, Li-Ion batteries are increasingly used in military and aerospace applications, and gradually moved to the fields of energy storage, electric vehicles (EV/PHEV/HEV). However, under conditions of high-rate charge and discharge, high tem-

* Corresponding author, e-mail: fanghale@163.com

perature working environment, local overheating caused by internal short circuit, component or battery failure, the exothermic reaction between the components of the battery accelerates, causing the temperature inside the battery to rise, this leads to a series of side effects. In the end, it may cause thermal runaway, and even battery burning and cracking [2-4].

At present, some researchers have studied the temperature field analysis of power batteries. Ni and Wang [5] conducted a characteristic test of a Li-Ion battery at various environment temperatures to study the best variation range of battery temperature, optimizing the heat dissipation of the battery pack at varying ambient temperatures. Leire *et al.* [6] set up a thermal generation model, and successfully calculated the thermal density of power battery, determined the optimal position of the temperature sensor, and the fan pulse modulation level was automatically adjusted. Li *et al.* [7] proposed an impedance-based method to describe the heat generation of battery in the process of overcharging, and proposed pulse-relaxation and impedance measurement methods, parameterizing the electro-thermal model on the different state of charge (SOC), temperature and charging rate. Authors in [8-11] researched into the thermal behavior of Li-Ion battery in various thermal environments and rejection of heat, and studied the relationship between failure form and internal reaction of Li-Ion battery through thermal abuse test. Zhu *et al.* [12, 13] investigated the thermal runaway characteristics of Li-Ion batteries under overcharging conditions and analyzed the temperature changes at different current rates and charging stages.

The aforementioned studies only consider the heating effect of the battery core, and ignore the Joule heat generated by the internal resistance of the battery poles itself when the current flows. At present, there are few related literatures in such research. According to temperature rise characteristics inside the battery, considering the thermal effects of the anode and cathode, Liu *et al.* [14] established a time-varying internal heat source model of heat generation rate, and obtain a more accurate battery temperature field distribution and its dynamic changes. Wu *et al.* [15] extracted the main characteristics of temperature distribution and heat generation rate distribution of stacked batteries based on numerical thermal simulation results, and discussed the thermal characteristics of batteries under different cell sizes and polar arrangements.

After the mentioned research, researchers have caught sight of that the polarity heating of battery is closely related to the temperature field distribution of the battery. The existing researches mostly analyze the heat dissipation and cooling of the battery module by air cooling, liquid cooling or coupling, and try to use the new cooling. Techniques such as PCM and heat pipes are used to cool battery modules [16-18], some attempts have been made to build battery thermal management systems on the basis of heat pipes, cooling is done by using phase change materials or microchannel cold plates [19-24], the overall method of battery heat dissipation is focused on by most researchers, but studies on localized heat dissipation for Li-Ion battery polar are rarely mentioned.

In order to deeply explore the influence of battery's two poles enhancement heat dissipation on Li-Ion battery, and to verify the method of enhancing the performance of the battery by improving the local heat dissipation conditions. In this paper, heat generation model of Lithium batteries with different discharge ratios is proposed, based on the characteristic of battery resistance changing with temperature and battery charged state, and coupled with the thermal effect of battery's two poles. Based on this model, the discharge process of single cell 1C and 2C was simulated. The contrast experiment of multiple rate discharge was carried out by setting the local heat dissipation structure in the positive and negative poles, the effects of local enhanced heat dissipation of pole ear on discharge performance and temperature distri-

bution of Li-Ion batteries were studied. According to the thermal characteristics of Li-Ion batteries and analysis results of local enhanced heat dissipation, a new battery module was designed. The design was simulated and tested by prototype experiment.

Establishment of battery heat generation model

Thermal parameter determination

The 3.7 V/50 Ah ternary Li-Ion power battery prepared by Jiangsu Huadong Lithium-ion Battery Technology Research Institute was used as the test object. Use Arbin's EVTS-174075-T-72KVA-IGBT battery test bench and high and low temperature test chamber to test the battery capacity, the internal resistance of battery charge and discharge and the voltage curve of battery open circuit under different temperature. Ten batches of this batch of batteries were measured and averaged to obtain their structural parameters, as shown in tab. 1.

Table 1. Battery structure parameters

Parameter	Average value	Parameter	Average value
Electrical core capacity [Ah]	53.0	Positive polar width [mm]	50
Electrical core thickness [mm]	7.115	Positive polar thickness [mm]	0.2
Electrical core width [mm]	347.0	Positive polar weight [g]	1.287
Electrical core length [mm]	196.0	Negative polar length [mm]	42
Electrical core weight [g]	1057.6	Negative polar width [mm]	50
Weight energy density [Whkg ⁻¹]	184.5	Negative polar thickness [mm]	0.2
Positive polar length [mm]	42	Negative polar weight [g]	4.321

The internal resistance of the ternary Li-Ion battery of 10 °C, 30 °C, and 50 °C was measured by the mixed pulse power characteristic step method [25], and parameters are 120 seconds and 0.5C. The calculation results are illustrated in fig. 1.

When measuring the batteries' internal resistance, its SOC-OCV curve can be obtained at the same time. The SOC-OCV curve obtained by measurement during battery discharge at 10 °C, 30 °C, and 50 °C is shown in fig. 2.

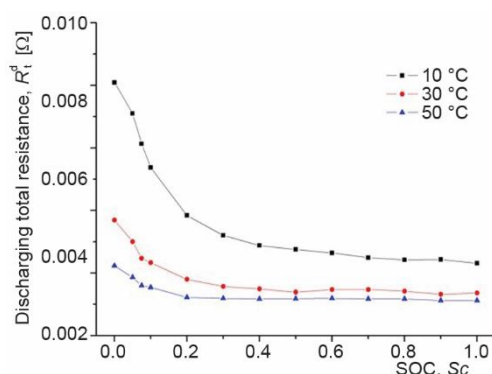


Figure 1. Diagram of battery discharging total resistance and SOC under three different temperature conditions

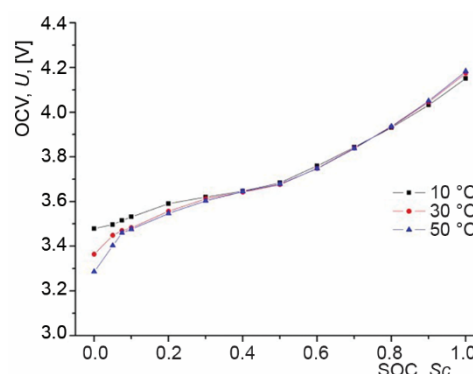


Figure 2. Battery discharging SOC-OCV diagram under three different temperature condition

Electrical core heat generation models

According to the Bernardi heat model [26], the heat production rate of the battery is calculated:

$$Q = q_{\text{rev}} + q_{\text{irev}} + q_{\text{CC},p} + q_{\text{CC},n} \quad (1)$$

$$q_{\text{rev}} = -\frac{J}{2} \frac{1}{d_{\text{PE}} + d_{\text{S}} + d_{\text{NE}}} T \frac{\partial U_{\text{OC}}}{\partial T} \quad (2)$$

$$q_{\text{irev}} = \frac{J}{2} \frac{1}{d_{\text{PE}} + d_{\text{S}} + d_{\text{NE}}} (U_{\text{OC}} - \Phi_{\text{p}} + \Phi_{\text{n}}) = \frac{J^2 R}{2} \quad (3)$$

$$q_{\text{CC},j} = \frac{\sigma_j (\nabla \Phi_j)^2}{2} \quad (4)$$

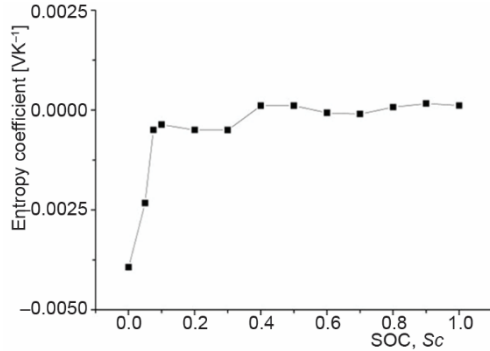


Figure 3. The variation trend of entropy thermal coefficient with charge state

where q_{rev} [Wm^{-3}] is the reversible heat production rate, q_{irev} [Wm^{-3}] – the irreversible heat production rate, $q_{\text{CC},j}$ [Wm^{-3}] – the ohmic heat production rate on the current collector, $q_{\text{CC},p}$, $q_{\text{CC},n}$ [Wm^{-3}] – the ohmic heat production rate on the current collector at the positive and negative poles, d_{PE} , d_{S} , d_{NE} [m] – the thickness of the anode, the separator, and the cathode, respectively, $(\partial U_{\text{OC}})/\partial T$ [VK^{-1}] – the entropy thermal coefficient of the battery, and U_{OC} – the open-circuit voltage (OCV). The function shown in fig. 3 is the entropy heat coefficient obtained by experimental measurement as the charge state.

The thermal parameter estimation method for superimposed Li-Ion batteries proposed by Wu *et al.* [27], by means of contrasting the simulation results with the results of experimental, the thermal model parameters of the ternary Li-Ion cell used in this study can be obtained, as shown in tab. 2. Further assume that the heat generation rate within the core plane is evenly distributed. In order to calculate the variation law of battery core heat generation rate with time under each discharge rate, a polynomial fit was performed on the relationship between internal resistance and entropy heat coefficient at 30 °C with SOC, figs. 1 and 3. Ignoring the effect of temperature on irreversible heat and reversible heat, the heat yield of the core at different discharge rates can be expressed as the following polynomial:

$$q(t) = I^2 R(t_{\Delta}) - IT \frac{\partial U}{\partial T}(t_{\Delta}) = \sum_{n=0}^7 a_n t_{\Delta}^n \quad (5)$$

where $t_{\Delta} = t/t_i$ is the proportion of the discharged time to the total discharge time, and a_n obtained by curve fitting. Table 3 gives the curve fitting parameters for different discharge rates.

Table 2. Thermal model parameters of Li-Ion battery cores

Parameter	Value
Thermal conductivity in the plane of the core [$\text{Wm}^{-1}\text{K}^{-1}$]	21
Thermal conductivity of vertical core plane [$\text{Wm}^{-1}\text{K}^{-1}$]	0.48
Core specific heat capacity [$\text{Jkg}^{-1}\text{K}^{-1}$]	1243
Battery core density [kgm^{-3}]	2300
Convective heat transfer coefficient [$\text{Wm}^{-1}\text{K}^{-1}$]	3.5

Table 3. Curve fitting parameters at different discharge rates

Magnification	1C	2C	Magnification	1C	2C
a_0	1.81	10.43	a_4	-1306.69	578.40
a_1	-94.58	-209.25	a_5	14570.92	25290.29
a_2	1038.22	2360.81	a_6	-19497.99	-36691.91
a_3	-2754.45	-6882.82	a_7	8113.97	15705.02

Battery polarity heat effect generation models

In the polar region, both the resistance of the poles and the contact resistance between the poles and the wires are the cause of the heat generation:

$$Q = q_{\text{tab},j} \tag{6}$$

$$q_{\text{tab},j} = \left(\frac{I_{\text{tab}}}{A_{\text{tab},j}} \right)^2 \left(\frac{1}{\sigma_{\text{tab},j}} + \frac{1}{\sigma_{\text{c},j}} \right) \tag{7}$$

where I_{tab} [A] is the current through the polar, $A_{\text{tab},j}$ [m^2] – the cross-sectional area of the polar, $\sigma_{\text{tab},j}$ [Sm^{-1}] – the conductivity of the polar material, and $\sigma_{\text{c},j}$ [Sm^{-1}] – the converted conductivity of the contact resistance at the polar and the wire. The parameters of the ternary Li-Ion battery polarity heat effect generation model adopted in this paper are shown in tab. 4.

Table. 4 Thermal model parameters of Li-Ion battery polar

	Anode	Cathode
Polar thickness [mm]	0.2	0.2
Polar width [mm]	50	50
Polar length [mm]	42	42
Thermal conductivity [$\text{Wm}^{-1}\text{K}^{-1}$]	237	401
Specific heat capacity [$\text{Jkg}^{-1}\text{K}^{-1}$]	900	385
Density [kgm^{-3}]	2700	8700
Conductivity [Sm^{-1}]	$37.8 \cdot 10^6$	$59.6 \cdot 10^6$
Conversion conductivity of contact resistance [Sm^{-1}]	$70 \cdot 10^6$	$80 \cdot 10^6$

From tab. 4 and eq. (7), the heat production rate of the anode and cathode at different discharge rates can be calculated, as shown in tab. 5.

Table 5. Heat production rate of ternary Li-Ion battery polar under different discharge rates

Magnification	Anode heat production rate [Wm^{-3}]	Cathode heat production rate [Wm^{-3}]
1C	450000	320750
2C	1800000	1283000

Single battery simulation and experimental verification

Taking full account of the exothermic effects of the polar, the positive polar and negative polar are modeled separately to create a simplified model of the battery. The load is loaded by internal heat generation, and the heat production rate of the positive and negative polar are set according to tab. 5. The battery is placed in a static air, the external convection heat dissipation power of the outer surface is 3.5 W, and the environment temperature is 30 °C. The parameters of rest heat analysis refer to the previous results of the calculation. The heat generation rate of the battery was loaded with reference to tab. 3 and eq. (5). The temperature cloud of the battery under 1C and 2C discharge conditions can be solved separately in the ANSYS WORKBENCH transient thermal analysis module, as shown in fig. 4. The maximum temperature was found at the positive polar of Li-Ion battery, which was 33.4 °C and 44.8 °C, respectively.

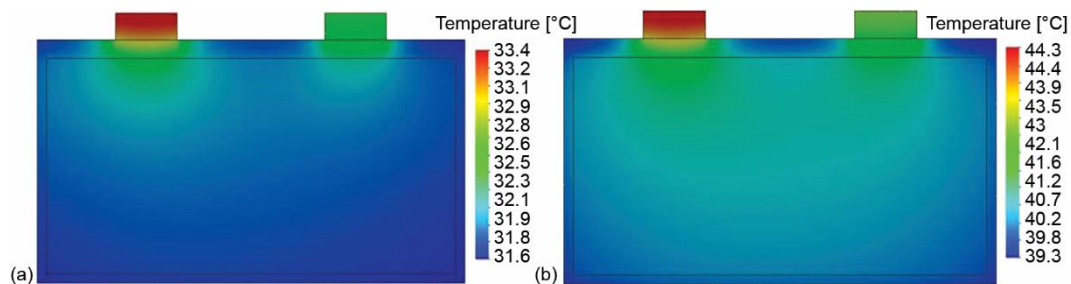


Figure 4. Temperature cloud charts at the end of the discharge; (a) 1C and (b) 2C

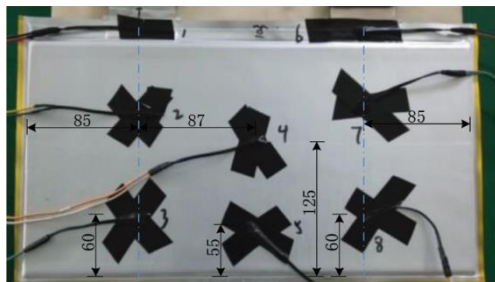


Figure 5. Temperature measurement point distribution map

The 1C and 2C discharge experiments were performed in the ternary Li-Ion battery at room temperature of 30 °C, and measured the battery's temperature. The distribution of the temperature measurement points is shown in fig. 5. The temperature values of the corresponding measuring points in the simulation analysis of 1C and 2C discharge processes are respectively extracted, as shown in fig. 6.

The temperature of the anode of the battery was measured by two sets of experiments, which were 33.3 °C and 43.4 °C, respectively.

The temperature of the corresponding positive ear measurement points in the simulation analysis were 33.4 °C and 44.7 °C, slightly higher than the experimental values. This is because

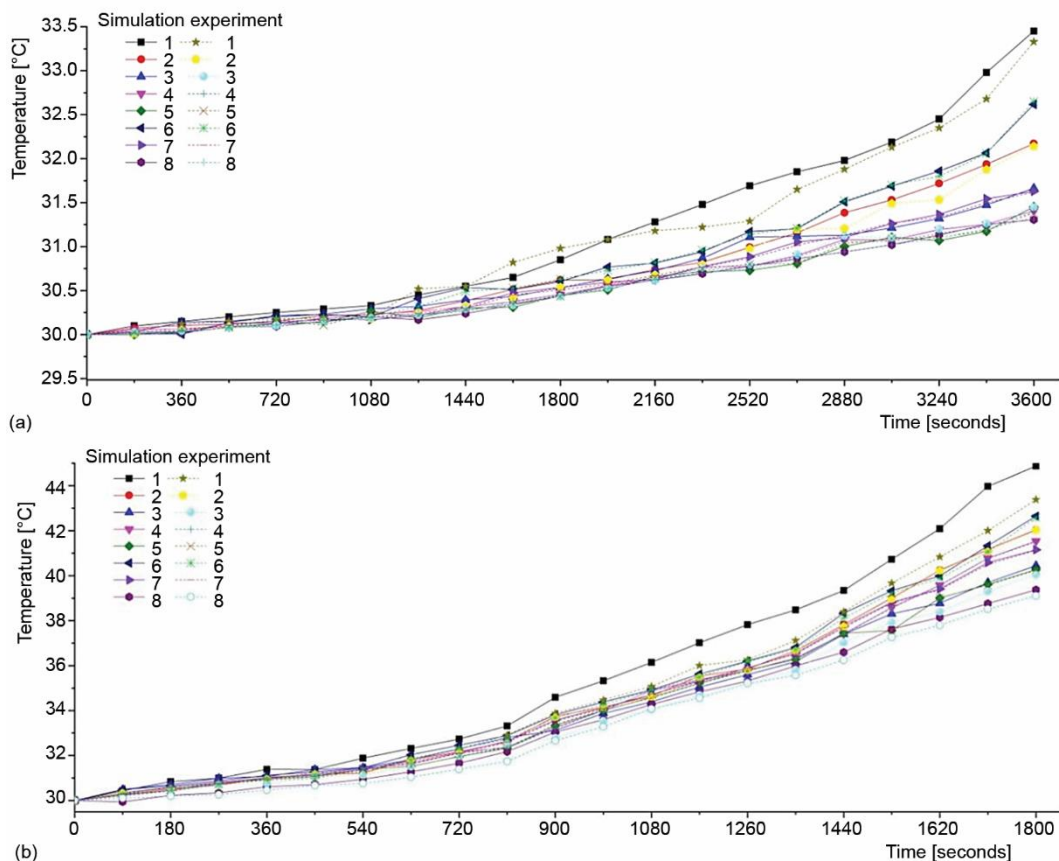


Figure 6. Comparison of single batteries' temperature measurement results; (a) 1C and (b) 2C

the copper charging clip with better thermal conductivity is used in the experiment, and the heat transfer efficiency is better than the natural convection heat that set in the simulation analysis. Through comparative analysis of simulation and experimental results, it is not difficult to find that the highest temperature of a single cell is in the positive ear, and the rise of ear canal temperature has great influence on the distribution of battery temperature field. It is necessary to model the polar ear separately and couple the thermal effects of the anode and cathode. The results of simulation analysis based on the heating model of Li-Ion battery are similar to the experimental temperature changing trend of each measuring point. Finite element analysis results are consistent with the experimental results, which can be used as a reference for thermal analysis of module discharge.

Polar enhanced heat analysis

The heating efficiency of the polar is obviously higher than that of the battery. To improve the heat dissipation efficiency and temperature distribution of Li-Ion batteries, heat pipes and fans are set at the positive and negative polar in this paper to discuss the influence of local enhanced heat dissipation on the discharge performance and temperature distribution of Li-Ion batteries.

Experimental procedure

- Select two batteries with the same charge and discharge performance and parameters in the batch of Li-Ion batteries, labeled 1# and 2#, respectively.
- One end of the heat pipe is in full contact with the fan and is fixed with tape, fix the other end at the polarity of the 1# battery, and make the polar and heat pipe fully contact with the thermal silica gel, T1 and T5 thermocouples are glued to the positive and negative poles respectively, and not contacted with the heat-conducting silica gel and heat pipe. Then fix the thermocouple to each point of the battery, as seen in fig. 7, the heat pipe and temperature measuring point arrangement is shown in fig. 8.
- Using the 2# battery as a reference, set the thermocouple at the same position on the surface (but no T7 survey mark), and the ambient temperature is 30 °C.
- Set the charge and discharge process: each process is charged to 4.2 V at 1C, discharged to 3.0 V, and the discharge process is set to 0.5C, 1C, 2C, 3C, 4C, 5C, 6C, 8C, 10C.
- After starting the program, record the data every 5 seconds.

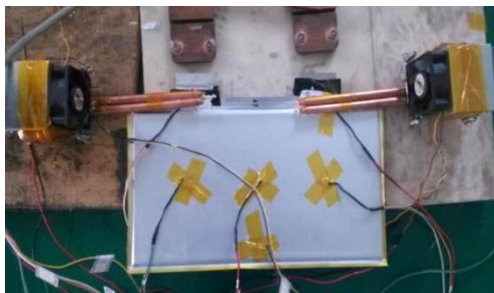


Figure 7. Locally enhanced heat dissipation experiment of the single battery

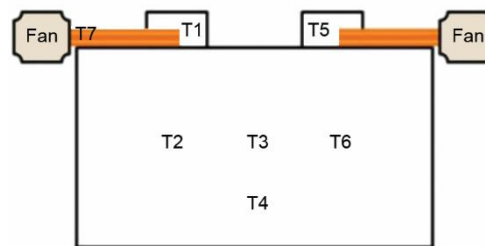


Figure 8. Layout of heat pipes and temperature measuring points

Analysis of the influence of single battery discharge rate performance

The discharge curves of the 1# Li-Ion battery with enhanced heat dissipation for the tabs and the 2# Li-Ion battery without heat dissipation at various magnifications are seen in figs. 9(a) and 9(b). According to the result, higher the discharge rate of a Li-Ion battery, the less energy it releases. Under rate of discharge 0.5C, the initial discharge voltage of the 1# Li-Ion battery is 4.17 V, and the cumulative discharge power is 51.35 Ah, which is slightly higher than the initial voltage of the 2# Li-Ion battery which is 4.13 V and the discharge capacity 49.04 Ah, at 1C rate of discharge. The discharge inception voltage of 1# Li-Ion battery is 4.11 V, and the accumulated discharge power is 50.07 Ah, which is also slightly higher than the initial voltage of 4.10 V and the discharge capacity of 48.67 Ah of the 2# Li-Ion battery. Under the 2C rate of discharge, the discharge inception voltage of 1# Li-Ion battery is 4.01 V, and the cumulative discharge power is 49.16 Ah, which is similar to the experimental result of the 2# Li-Ion battery. Under the 3C discharge rate, the initial discharge voltage of the 1# Li-Ion battery is 3.89 V, and the accumulated discharge power is 47.93 Ah, which is similar to the experimental result of the 2# Li-Ion battery. In the high-multiplier (4C, 5C, 6C, 8C, 10C) discharge experiment, with an increase in multiplier, the discharge inception voltage and the

cumulative discharge quantity of 1# Li-Ion battery are significantly reduced, but the corresponding experimental results are very similar to 2# Li-Ion battery.

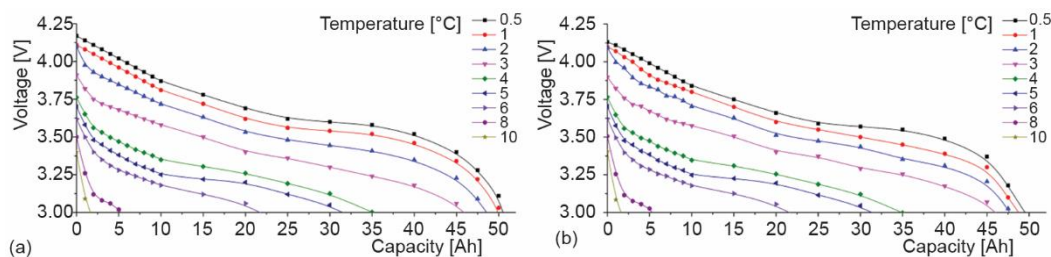


Figure 9. Discharge curves of single batteries at different discharge rates; (a) 1# enhanced heat dissipation battery and (b) 2# no enhanced heat dissipation battery

The safe working range of ternary Li-Ion battery is 4.2 V to 3.0 V. If the discharge is continued below 3.0 V, the battery will be damaged and the performance will be greatly attenuated. Therefore, 3.0 V is set as the protection cut-off voltage of the discharge test. The safe discharge capacity of the two batteries before reaching the protection cut-off voltage at each magnification is shown in fig. 10. It can be further found that under the 0.5C and 1C rate of discharge, the partial enhanced heat dissipation of the polar can slightly improve the safe discharge capacity of Li-Ion battery, and it can reach or even exceed the nominal value of 50 Ah. As the emission rate increases, the capacity retention rate of 1# Li-Ion battery and 2# Li-Ion battery tends to be similar. Especially in the high-power discharge experiments of 4C, 5C, 6C, 8C, and 10C, the safe discharge capacity of Li-Ion batteries will be significantly reduced whether or not the polar is strengthened for heat dissipation. At 4C discharge rate, the safe discharge capacity of Li-Ion batteries will be reduced to about 35 Ah, and the discharge velocity of the safe discharge capacity of Li-Ion battery has been reduced to below 5 Ah.

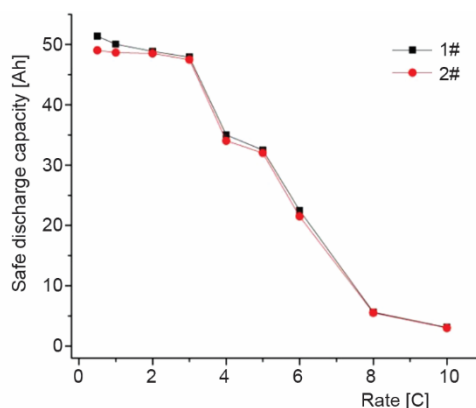


Figure 10. Safe discharge capacity of single batteries at different discharge rates

The Li-Ion battery internal resistance will be affected by temperature. To a certain extent, the internal resistance of the battery can be reduced by strengthening the heat dissipation of the polar region, and thus improve the initial voltage of discharge of the battery, so that the battery can release more electricity before reaching the protection cut-off voltage, thus improving the battery capacity. In the high-multiplier discharge experiment, the discharge current is large, while the reduction of battery internal resistance caused by partial intensification of heat dissipation of polar is small. Therefore, internal resistance of cell is still high, which has reached a protection cutoff voltage of 3.0 V before the end of the battery discharge, so it cannot improve the high-rate safety discharge capacity of the battery.

Influence on temperature distribution of single battery

The temperature distribution of 1# and 2# Li-Ion batteries after charging and discharge at each rate is shown in fig. 11. For the 2# Li-Ion battery without the ear-enhanced

heat dissipation, under different discharge rates, the hottest areas are at the positive end of the battery, and the areas with the second highest temperature are distributed in the negative polar of the battery. This is consistent with the simulation and experimental conclusions in section *Establishment of battery heat generation model*. As the emission rate increases, measure the temperature at T1 of the positive polar of Li-Ion battery keeps increasing. The highest temperature at 6C discharge rate is 62.3 °C, and then decreases rapidly. At 10C discharge rate, the temperature at T1 measuring point is 37.1 °C. Similarly, the value measured at each temperature point in the middle of the electrical core also increases as the discharge rate increases, reaching a maximum value of 57.7 °C at the 5C rate of discharge. The result of the previous experiment is that as the discharge rate increases, it is known from eq. (7), the rate of heat generation at the poles increases rapidly with the squared rate of discharge rate, and the battery cannot export the rapidly accumulated heat. Although its heat dissipation power increases with a rise in temperature, it is still inevitable that the temperature of polar will rise rapidly. It is also known from the experimental analysis in section *Analysis of the influence of single battery discharge rate performance* under the condition of high discharge speed, the capacity of Li-Ion battery is greatly reduced, and the accumulated heat is also reduced as the discharge time is shortened, which will lead to a limited temperature rise.

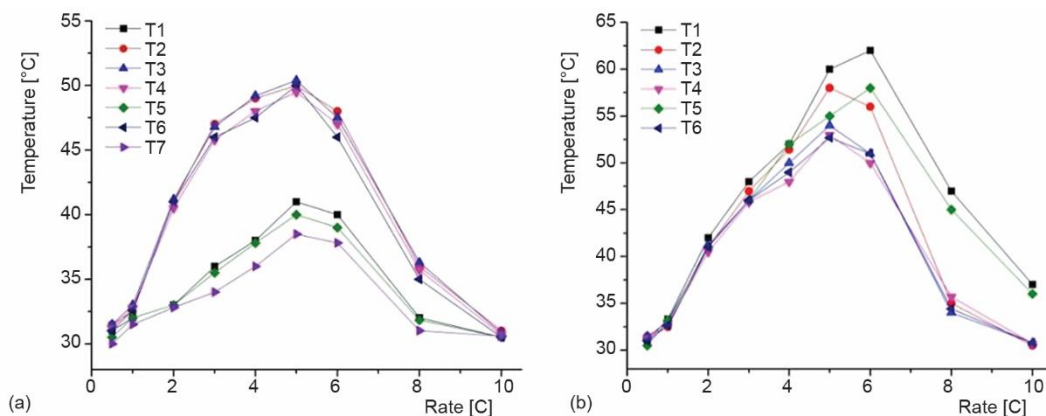


Figure 11. Temperature distribution of single batteries at different discharge rates; (a) 1# enhanced heat dissipation battery and (b) 2# no enhanced heat dissipation battery

For the 1# Li-Ion battery with enhanced battery polarity heat effect dissipation, the warmest regions occur in the center of the core, instead of the positive polar with the highest heat generation rate. The maximum temperature of 41.3 °C of positive and negative polar appeared at the discharge rate of 5C, which was nearly 20 °C lower than that of # 2 Li-Ion battery. It indicates that the heat generated by the polar regions can be quickly and efficiently deduced through heat pipes. With the increase of discharge rate, the temperature of each measurement point in the middle of the core increases continuously, and the change trend and amplitude are similar. The maximum temperature of 50.2 °C occurred at the 5C rate of discharge, which was 7.5 °C smaller than the temperature rise of the 2# Li-Ion battery. This indicates that the heat produced by the pole can exported in time through the heat pipe to reduce the heat transferred from the pole to the electrical core, thereby reducing the overall temperature rise of Li-Ion battery.

In summary, it can be found that Li-Ion batteries have a higher safe discharge capacity during low-rate (0.5C-3C) discharge. As the discharge rate increases, the safe discharge capacity of Li-Ion batteries will be greatly attenuated. Although the partial enhanced heat dissipation of the polar through heat pipe can only slightly improve the discharge capacity of Li-Ion battery at a low rate, it can timely and effectively export the heat generated by the polar, greatly reduce the polar temperature and the overall battery temperature, thus improving the thermal balance and safety performance of Li-Ion battery.

Module design and validation

Battery module structure design

According to the heating characteristics of the single battery and the requirements of the electric bus enterprises on the battery module capacity, the related battery module is designed, and the explosion diagram is shown in fig. 12. Multiple Li-Ion batteries eventually form each battery module and a plurality of heat dissipation partitions. The heat-dissipating partition is made of aluminum sheet metal stamping, and has a recessed area in the middle for accommodating the Li-Ion battery, and a folded edge on both sides to increase the heat-dissipating area. The heat pipe is bent into a C shape and placed in a receiving space formed by the edge of the Li-Ion battery and the heat dissipating partition. The heat generated is channeled with placing the long side of the heat pipe on one side of the battery ear by the tabs to the heat dissipation partitions and quickly dissipate. There are two side pressure plates on the outside of the battery module to fix and support the entire module. The whole module can be bundled or bolted into groups. For the sake of improve the heat dissipation capability and fixed reliability of Li-Ion battery, a thermal conductive silica gel is coated or filled between the contact faces of the Li-Ion battery and the heat dissipating partition plate. This can completely eliminate the air between the Li-Ion battery and the heat dissipation diaphragm. The temperature of thermal resistance is reduced and improves heat transfer performance. In addition, the thermal silica gel also helps to fix the single battery from vibration or shock.

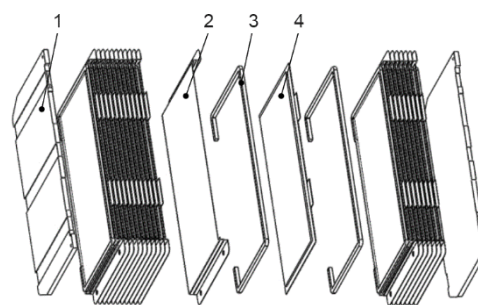


Figure 12. Schematic diagram of heat pipe setting; 1 – side pressure plate, 2 – heat dissipation partition, 3 – heat pipe, 4 – Li-Ion battery

Simulation and contrast analysis

To verify the impact partial heat dissipation of polar ear on the temperature field distribute over Li-Ion battery module, ANSYS WORKBENCH transient thermal analysis module was used to analyze the battery module with and without heat pipe, and solved the battery module temperature distribution problem when 1C and 2C end discharge. In the analysis, it is assumed that the battery and the separator are bonded together by a thermal conductive silica gel, and the adhesive layer is 0.1 mm. The 0.1 mm thick thermal silica material (Arctic Silver 5) has a heat transfer coefficient of approximately 35,000 W/Km². Then the distributed thermal resistance is the reciprocal of heat transfer coefficient: 1.143×10^{-5} Km²/W, the module

housing body forced convection cooling power is set to 30 W. For the remaining thermal analysis parameters, refer to the previous calculations for analysis results.

Figure 13 shows the temperature distribution of the heat pipe free battery modules 1C and 2C at the end of discharge (side platen is hidden). The hottest part of the battery is the middle part of the module, which is represented by an elliptical red area in the temperature cloud image, and the temperature gradually decreases toward both sides. In the 1C discharge simulation analysis, the maximum temperature at which the battery module present is 43.2 °C, the highest temperature rise was 13.2 °C, the difference between the highest and lowest temperature of the entire battery module is 7.9 °C. In the 2C discharge simulation analysis, the highest temperature of the battery module is 55.8 °C, the highest temperature rise was 25.8 °C, and the maximum temperature difference of the entire battery module was 21.9 °C.

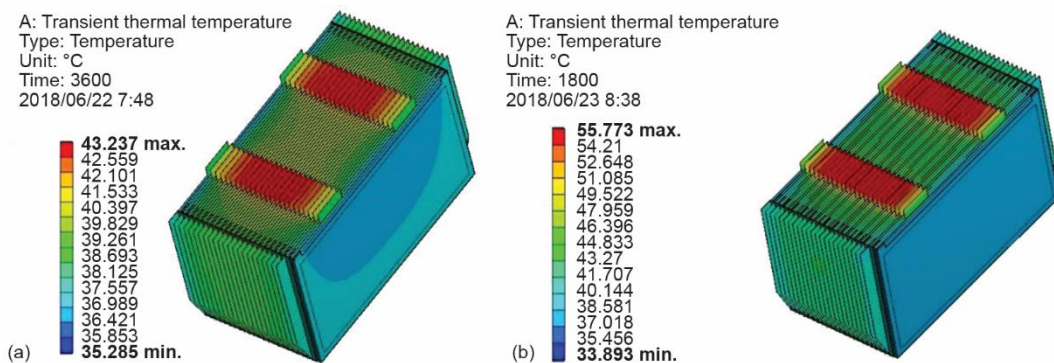


Figure 13. Temperature cloud charts of the module without heat pipes at the end of the discharge; (a) 1C and (b) 2C

The temperature distribution of the battery module is shown in fig. 14 at the end of 1C and 2C discharges (with side platen hidden) for the battery module with partial enhanced heat dissipation by polar. The highest temperature region is also situated in the center of the battery module, but the red area in the temperature cloud map is slightly increased compared with the no heat pipe module, the temperature value is reduced, and the overall temperature change gradient is reduced. The experimental results show that the heat generated can be effectively transferred by the heat pipe structure by the polar to the heat dissipation partition, and

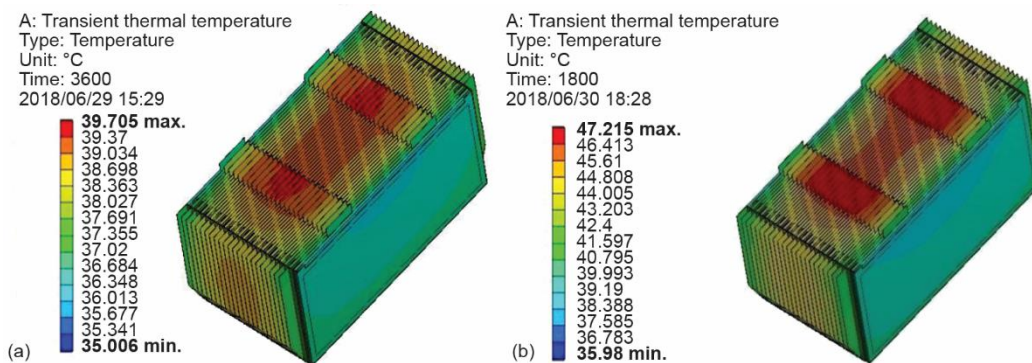


Figure 14. Temperature cloud charts of the module with heat pipes at the end of the discharge; (a) 1C and (b) 2C

and has a thermal equalization effect on the whole module. As shown in tab. 6, in the 1C discharge simulation analysis, the maximum temperature at which the heat pipe module present is 39.7 °C, the temperature rise is 9.7 °C, the difference between the highest and lowest temperature of the entire battery module is 4.7 °C, which is 3.2 °C lower than that of the module without heat pipe, the reduction is about 41.3%. In the 2C discharge simulation analysis, the maximum temperature at which the heat pipe module present is 47.2 °C, the temperature rise is 17.2 °C, the difference between the highest and lowest temperature of the entire battery module is 11.2 °C, which is 10.7 °C lower than that of the module without heat pipe, and the reduction is about 48.9%. This shows that the heat pipe enhanced heat dissipation structure has good heat dissipation performance and thermal balance performance, which can the temperature difference between the batteries and the absolute temperature rise of the battery module be reduced. It can also be found that in the 1C and 2C discharge simulation analysis, the temperature of the folded edge on both sides of the heat dissipation partition is only 2-3 °C lower than the maximum temperature of the module. This indicates that the heat from the polar body can be conveyed via the heat pipe structure to the edge of the cooling baffle. If the heat exchange between the folded edges of the heat dissipation baffle and the outside can be enhanced to the absolute temperature rise of the battery module can be further reduced by improving the convective heat dissipation capacity. Therefore, when designing the battery box, the air duct requires to be optimized render certain that the outer surface of the battery module has a high convection heat dissipation power, thereby ensuring that the heat conducted by the heat pipe structure can be dissipated in time.

Table 6. Comparison of temperature analysis results of battery modules

	1C	2C
The maximum temperature of module without heat pipe	43.2 °C	55.8 °C
The minimum temperature of module without heat pipe	35.3 °C	33.9 °C
No heat pipe module temperature difference	7.9 °C	21.9 °C
The maximum temperature of the heat pipe module	39.7 °C	47.2 °C
The minimum temperature of the heat pipe module	35.0 °C	36.0 °C
Heat pipe module temperature difference	4.7 °C	11.2 °C
Temperature reduction range	40.5%	48.9%

Experimental verification

The battery module prototype was completed and prototyped, as shown in fig. 15. 1C and 2C relevant experiments performed carried out on the battery module at room temperature of 30 °C and under the condition of enhanced convection heat dissipation, and thermocouples were set inside the module and at the pole ears of each battery to measure the module temperature. The distribution of temperature measurement points is shown in fig. 16.

Figure 17 shows the temperature change trend of each temperature measurement point of the battery module. In the 1C discharge experiment, the temperature rise of the No. 5 measuring point is the largest, which is 10.4 °C, and the temperature rise of the No. 1 and No. 11 measuring points is small, which is 4.8 °C, the difference between the highest and lowest temperature of each point is 11.2 °C. Similar to the 1C discharge experiment, in the 2C discharge experiment, the maximum temperature rise was 19.5 °C at measuring point No. 5, and the

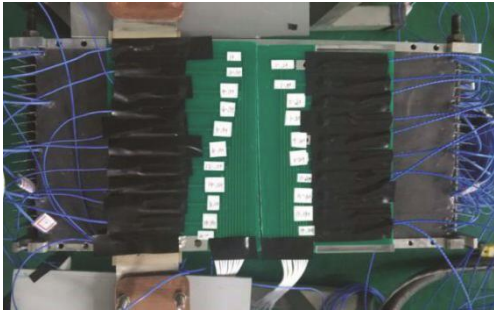


Figure 15. Experimental diagram of battery module prototype

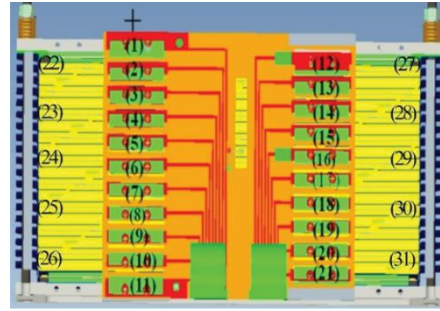
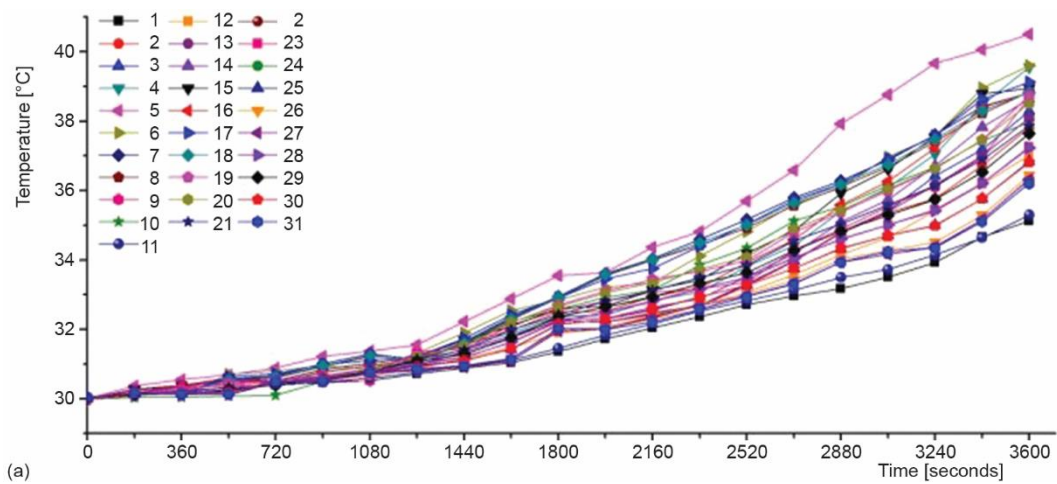
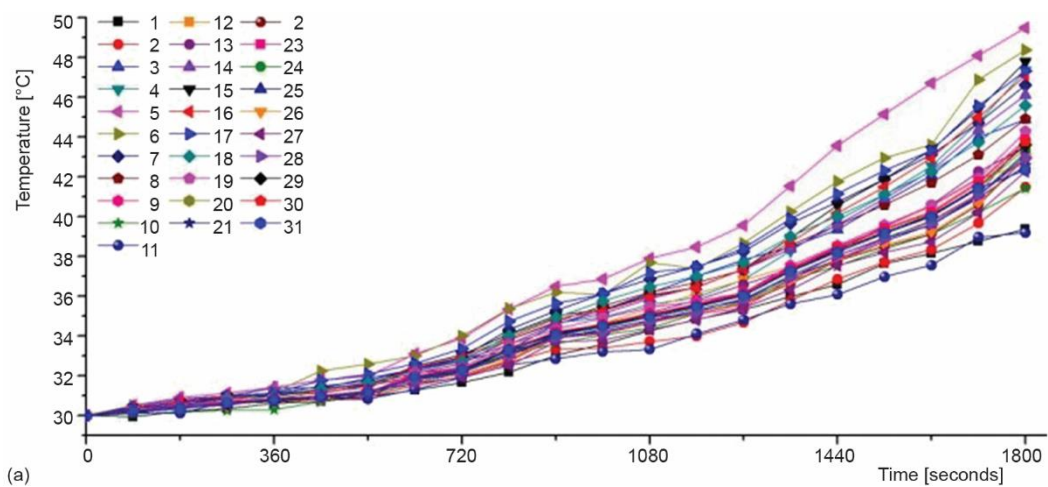


Figure 16. Temperature distribution diagram of the module



(a)



(a)

Figure 17. Comparison of modules' temperature measurement results; (a) 1C and (b) 2C

temperature rise of the No. 11 measuring point was small, 9.2 °C, and the maximum temperature difference of each measuring point was 10.3 °C. The experimental results are generally similar to the simulation analysis results above, but the maximum temperature measured by this module is slightly higher than the simulation result, and the temperature rise of the total positive pole is lower and the total negative polar is lower than that of the simulation results. The reasons for this phenomenon are:

- No. 1 and No. 11 measuring points are located at the total positive pole and the total negative pole of the module respectively. They are all laser welded with a single material, and the contact resistance is low, thus reducing the heat production rate.
- No. 1 and No. 11 measuring points are located outside the module, and the heat dissipation condition is good, so the temperature is low.
- The measuring point No. 5 is located in the center of the module, and the heat dissipation condition is poor.

After inspection, it is found that the welding strength of the polar is weak, and the contact resistance is large, which also causes the heat to be relatively large.

To sum up, the measured results in the experiment are similar to the simulation analysis results of the module, indicating that the Li-Ion battery heat generation model coupled with the positive and negative polar heat effects can be used for module discharge thermal analysis. The localized heat dissipation of the polar can quickly transfer the heat of the ear to the edge of the heat dissipating baffle, which has good heat dissipation performance and thermal balance performance, and can effectively decrease the absolute heat rise of the battery module and the temperature difference between the batteries. When designing the battery box, the air duct needs to be optimized to ensure that the outer surface of the battery module has a high convection heat dissipation power, thereby ensuring that the heat conducted by the heat pipe structure can be dissipated in time. When manufacturing a Li-Ion battery module, it is necessary to ensure the welding effect of the tabs, otherwise the contact resistance will be increased, thereby affecting the heat generation rate.

Conclusions

In this paper, in order to deeply explore the influence of polar enhancement heat dissipation on Li-Ion battery, the thermal effect of anode and cathodes were coupled, and the heat generation model under different ratios was proposed, and the comparison was made through multi-ratio discharge experiments. Then, a local heat dissipation structure was set up and the thermal analysis and comparison of battery module discharge simulation were carried out. Finally, according to the thermal characteristics and the results of locally enhanced heat dissipation analysis, a new battery module is designed and simulated. The prototype is completed and tested.

The main breakthrough points solved in this paper are as follows.

- Although the partial enhanced heat dissipation of the polar through heat pipe can only slightly improve the discharge capacity of Li-Ion battery at a low rate, it can timely and effectively export the heat generated by the polar, greatly reduce the temperature at the polar and the overall temperature of the battery, thus improving the thermal balance and safety performance of Li-Ion battery.
- The heat dissipation structure is strengthened at the pole, which can transmit the heat generated by the polar ear to the heat dissipation partition in time, and the absolute temperature rise of the battery module and the temperature difference between the batteries be effectively reduced

- When manufacturing a Li-Ion battery module, it is necessary to ensure the welding effect of the polar to reduce the contact resistance, thereby avoiding the excessive heat generation rate of the polar. When designing the battery box. It is necessary to optimize the air duct to ensure that the outer surface of the battery module has high convective heat dissipation capacity, thereby ensuring that the heat conducted by the heat pipe structure can be dissipated in time.

Acknowledgment

This work is financially supported by Jiangsu Science and Technology Infrastructure Program (Grant No. BE2014006-2) and General program of natural science research in Jiangsu Province universities (Grant No. 17KJB480004).

References

- [1] Kim, J., et al., Review on Battery Thermal Management System for Electric Vehicles, *Applied Thermal Engineering*, 149 (2019), Feb., pp. 192-212
- [2] Yuan, L., et al., Experimental Study on Thermal Runaway and Vented Gases Of Lithium-Ion Cells, *Process Safety and Environmental Protection*, 144 (2020), Dec., pp. 186-192
- [3] An, Z., et al., Modeling and Analysis of Thermal Runaway in Li-Ion Cell, *Applied Thermal Engineering*, 160 (2019), Sept., pp. 113960
- [4] Quintiere, J. G., On Methods to Measure the Energetics of a Lithium Ion Battery in Thermal Runaway, *Fire Safety Journal*, 111 (2019), Jan., ID 102911
- [5] Ni, P. Y., Wang, X., Temperature Field and Temperature Difference of a Battery Package for a Hybrid Car, *Case Studies in Thermal Engineering*, 20 (2020), Aug., ID 100646
- [6] Leire, M.-M., et al., Optimization of Thermal Management Systems for Vertical Elevation Applications Powered by Lithium-Ion Batteries, *Applied Thermal Engineering*, 147 (2018), Jan., pp. 155-166
- [7] Li, J. Q., et al., Lithium-Ion Battery Overcharging Thermal Characteristics Analysis and an Impedance-based Electro-Thermal Coupled Model Simulation, *Applied Energy*, 254 (2019), Nov., ID 113574
- [8] Gao, T. F., et al., Hazardous Characteristics of Charge and Discharge of Lithium-Ion Batteries Under Adiabatic Environment and Hot Environment, *International Journal of Heat and Mass Transfer*, 141 (2019), Oct., pp. 419-431
- [9] Wang, Z. R., et al., Calculation Methods of Heat Produced by a Lithium-Ion Battery Under Charging-Discharging Condition, *Fire and Materials*, 43 (2019), 2, pp. 219-226
- [10] Guo, L. S., et al., Effects of the Environmental Temperature and Heat Dissipation Condition on the Thermal Runaway of Lithium Ion Batteries During the Charge-Discharge Process, *Journal of Loss Prevention in the Process Industries*, 49 (2017), Sept., pp. 953-960
- [11] Jiang, F. W., et al., Theoretical Analysis of Lithium-Ion Batteries Failure Characteristics Under Different States of Charge, *Fire and Materials*, 42 (2018), 6, pp. 680-686
- [12] Zhu, X. Q., et al., Overcharge Investigation of Large Format Lithium-Ion Pouch Cells with Li(Ni_{0.6}Co_{0.2}Mn_{0.2})O₂ Cathode for Electric Vehicles: Degradation and Failure Mechanisms, *Journal of The Electrochemical Society*, 165 (2018), 16, pp. A3613-A3629
- [13] Zhu, X. Q., et al., Overcharge Investigation of Large Format Lithium-Ion Pouch Cells with Li(Ni_{0.6}Co_{0.2}Mn_{0.2})O₂ Cathode for Electric Vehicles: Thermal Runaway Features and Safety Management Method, *Energy*, 169 (2019), Feb., pp. 868-880
- [14] Liu, F. F., et al., Simulation and Experiment on Temperature Field of Lithium-ion Power Battery for Vehicle Based on Characteristic of Dynamic Heat Source, *Journal of Mechanical Engineering*, 52 (2016), 8, pp. 141-151
- [15] Wu, B., et al., Thermal Design Optimization of Laminated Lithium Ion Battery Based on the Analytical Solution of Planar Temperature Distribution, *SCIENCE CHINA Technological Sciences*, 44 (2014), 11, pp. 1154-1172
- [16] Hu, Q. W., et al., Review on Cooling Technique for Li-Ion Battery Pack, *Marine Electric & Electronic Engineering*, 36 (2016), 2, pp. 53-58
- [17] Zhang, T. S., et al., Numerical Model And Computational Analysis On Battery Thermal Management System With Heat Pump Auxiliary Cooling, *Acta Energetica Solaris Sinica*, 39 (2018), 3, pp. 713-721

- [18] Lei, S. G., *et al.*, Collaborative Analysis of Heat Transfer Enhancement of SiO₂ Nanofluids and High Concentration Cell Cooling, *Proceedings of the CSEE*, 36 (2016), 12, pp. 3285-3292
- [19] Rao, Z. H., *et al.*, Experimental Investigation on Thermal Management of Electric Vehicle Battery with Heat Pipe, *Energy Conversion and Management*, 65 (2013), Jan., pp. 92-97
- [20] Zhao, J. T., *et al.*, Experimental Study on the Thermal Management Performance of Phase Change Material Coupled with Heat Pipe for Cylindrical Power Battery Pack, *Experimental Thermal and Fluid Science*, 82 (2017), Apr., pp. 182-188
- [21] Huo, Y. T., *et al.*, Investigation of Power Battery Thermal Management by Using Mini-Channel Cold Plate, *Energy Conversion and Management*, 89 (2015), Jan., pp. 387-395
- [22] Wang, Q. C., *et al.*, Thermal Performance of Phase Change Material/Oscillating Heat Pipe-Based Battery Thermal Management System, *International Journal of Thermal Sciences*, 102 (2016), Apr., pp. 9-16
- [23] Tran, T. H., *et al.*, Experimental Investigation on the Feasibility of Heat Pipe Cooling for HEV/EV Lithium-Ion Battery, *Applied Thermal Engineering*, 63 (2014), 2, pp. 551-558
- [24] Greco, A., *et al.*, A Theoretical and Computational Study of Lithium-Ion Battery Thermal Management for Electric Vehicles Using Heat Pipes, *Journal of Power Sources*, 257 (2014), July, pp. 344-355
- [25] Sato, N., Yagi K., Thermal Behavior Analysis Of Nickel Metal Hybrid Batteries Vehicles, *J. SAE Review*, 21 (2000), 2, pp. 205-211
- [26] Bernardi, D., *et al.*, A General Energy-Balance for Battery Systems, *J. Electrochem Soc*, 132 (1985), 1, pp. 5-12
- [27] Wu, B., *Thermal Design Methodology for Traction Lithium-Ion Batteries*, Tsinghua University, Beijing, China, 2015